

BLOCK GENERALIZED SPATIAL MODULATION FOR MASSIVE MIMO SYSTEMS

Elam Curry and Deva K. Borah

Klipsch School of Electrical & Computer Engineering

New Mexico State University

Las Cruces, NM 88003, USA

email: mrelam1@nmsu.edu, dborah@nmsu.edu

Faculty Advisor:

Deva K. Borah

ABSTRACT

Spatial modulation techniques have the ability to convey information by both the positions of active antennas as well as the symbols they transmit. Such techniques include the generalized spatial modulation (GSM) that can provide high spectral efficiency. In general, however, the total number of available symbols in GSM is not a power of two. Therefore, selection of a symbol alphabet from the available symbols is needed. This is a numerically complex problem. In this paper, we propose to significantly reduce the complexity of the GSM symbol set selection problem by grouping antennas together to form blocks, thus producing block GSM (BGSM) symbols. A previously developed iterative combinatorial method is extended to BGSM symbol selection. The effects of the Rician K-factor, BGSM symbol block size, and antenna configuration on the performance and design complexity are studied. The algorithm is found to significantly reduce the complexity of the BGSM symbol set selection problem.

INTRODUCTION

Large scale multiple input multiple output (MIMO) systems have been receiving increased attention due to their ability to support the advent of 5G networks. Such systems provide multiple advantages, such as increased link reliability, improved spectral efficiency, higher directivity, and improved power efficiency [1], [2]. However, the use of MIMO systems always comes at the cost of new challenges, such as antenna correlation, more radio frequency (RF) transmitter chains, increased communication design complexity, and increased hardware complexity. A class of modulation techniques that can exploit the benefits of MIMO systems while simultaneously reducing the number of RF transmit chains is the broad category of spatial modulations.

Notable modulation techniques of the spatial modulation class include spatial modulation (SM), generalized space-shift keying (GSSK), and generalized spatial modulation (GSM). In GSSK, N_a out of N_t total antennas are made active in each channel use. Information is conveyed solely by

the positions of the active antennas in this modulation technique. In SM, only one antenna is made active in each channel use. The active antenna transmits a symbol from a quadrature amplitude modulation (QAM) alphabet. The SM modulation technique benefits from only needing one transmit processing chain, but is generally outperformed by GSM. In GSM, N_a out of N_t total antennas are made active in each channel use, and each active antenna transmits a symbol from an M -QAM alphabet. This gives GSM the highest spectral efficiency within the modulation class discussed here, but at the cost of increased complexity. In GSM, the total number of symbols to select from is $C = M^{N_a} \binom{N_t}{N_a}$. The number of symbols selected for communication C' is typically a power of two so that $r = \log_2(C')$ bits per channel use (bpcu) is an integer. This gives rise to the problem of selecting a set of C' symbols from a total of C symbols. For most practical scenarios, the problem of examining $\binom{C}{C'}$ symbol sets is far too complex to be solved by any exhaustive search technique. In [3], a symbol set selection tree is developed to solve the symbol set selection problem for visible light communication (VLC) GSSK systems. A direct extension of this tree to GSM systems would be prohibitively complex. Later in [4], a similar tree is developed to solve the symbol set selection problem in VLC GSM systems. While a tree search provides an optimal solution, the complexity is prohibitively high for most practical scenarios. Thus, a low complexity iterative combinatorial generalized spatial modulation (ICGSM) method is developed in [5] to solve the GSM symbol set selection problem with manageable complexity. While the ICGSM can solve the symbol selection problem for moderate size systems, further reduction in complexity is necessary when the problem becomes larger, for example, when massive MIMO is employed.

In this paper, we propose a block based GSM symbol selection algorithm by grouping multiple antennas together to act as one transmit antenna. Each antenna in an antenna group transmits the same symbol. Accordingly, a block iterative combinatorial generalized spatial modulation (BICGSM) algorithm is developed based on the original ICGSM algorithm. The BICGSM algorithm obtains a set of locally optimal symbols to use for transmission. The proposed BICGSM approach offers drastically reduced complexity and improved symbol error rate (SER) performance for similar RF chains. The SER performance of the BICGSM is investigated for both line-of-sight (LOS) and Rician channel conditions. The effect of transmitter antenna configuration on SER performance is also studied.

Notations: We use bold lower case letters for column vectors, and bold upper case letters for matrices. For a set of vectors, \mathbf{b}_i denotes the i -th vector, and $b_{i,m}$ is the m -th element of vector \mathbf{b}_i . For a matrix \mathbf{A} , $A_{m,n}$ denotes the (m, n) -th element and $\mathbf{A}^{1/2}$ denotes its square root. For a set Ω , $|\Omega|$ denotes its cardinality. The notations $[\cdot]^T$, $[\cdot]^H$, $\|\cdot\|_l$, and $E[\cdot]$ denote transpose, the Hermitian operator, the l -norm, and expectation respectively. We denote $\binom{n}{k}$ as $n!/(n-k)!k!$ and $\mathcal{CN}(m, \sigma^2)$ as the complex Gaussian distribution with mean m and variance σ^2 .

MIMO CHANNEL MODEL

We consider a MIMO system with N_t transmit antennas and N_r receive antennas. For simplicity, we consider $N_r = 2$, although the algorithm can be applied to any number of receive antennas. In this paper, we investigate both a uniform rectangular array (URA) and a uniform linear array (ULA), which is a special case of the URA with a single row. The distances between adjacent antennas in the transmitter and receiver arrays are d_t and d_r respectively. The transmit array is allowed to have

any orientation, and the axes are chosen so that the transmit array is confined to the x - z plane as shown in Fig. 1. For simplicity, the transmitter and receiver arrays are kept parallel. The distance between the lower corner antennas of the transmit and receive arrays is R as shown in Fig. 1

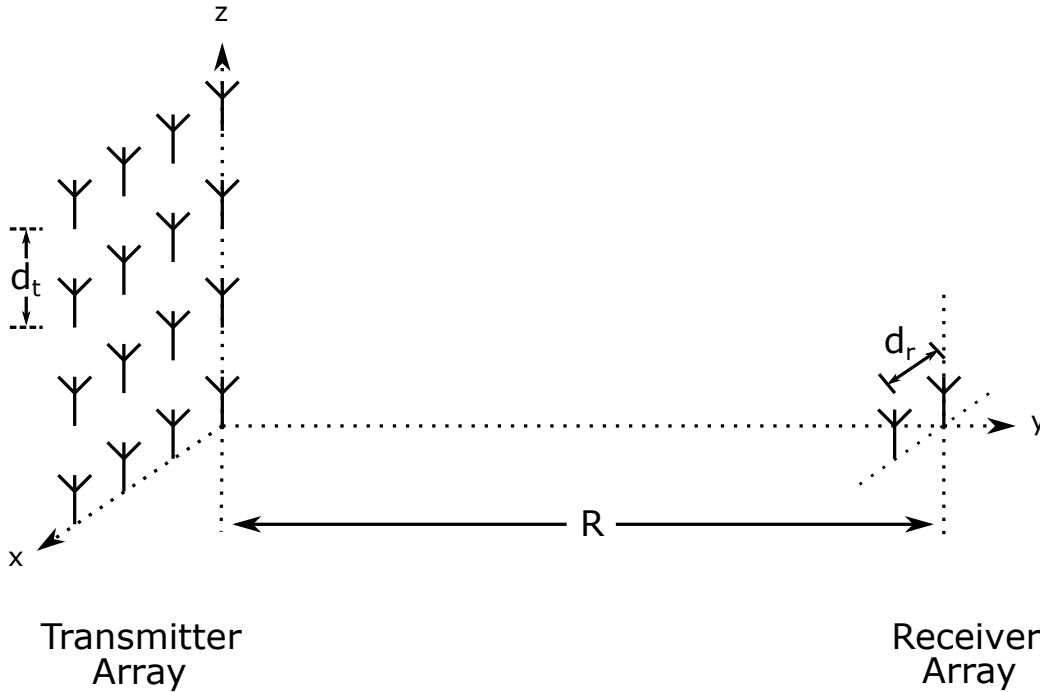


Figure 1: An example of a MIMO system with $N_t = 16$ transmit antennas and $N_r = 2$ receive antennas.

In GSM systems, only N_a out of N_t antennas are activated in each channel use. Each of the activated antennas transmits a QAM symbol from an M -QAM alphabet \mathcal{B} . We denote $\mathbf{u} = [u_1, \dots, u_{N_t}]^T$ as GSM symbol, where $u_i \in \mathcal{B}$ if antenna i is active, and $u_i = 0$ otherwise. The received signal vector is modeled as

$$\mathbf{y} = \gamma \mathbf{H} \mathbf{u} + \mathbf{n}, \quad (1)$$

where \mathbf{H} is the channel matrix with each element $H_{i,j}$ representing the channel between transmit antenna j and receive antenna i , \mathbf{n} is the i.i.d. complex Gaussian noise vector with $n_i \sim \mathcal{CN}(0, \sigma^2)$, σ^2 is the noise variance at each receiver antenna, $\gamma = 1/\sqrt{E[\mathbf{u}_i^H \mathbf{u}_i]}$ is a transmit power normalization constant, and $E[\cdot]$ denotes averaging over the selected symbol set Ω . The constant γ is needed because different symbol sets Ω may result in different average symbol energy values. The channel matrix is modeled as Rician and is given by [6], [7],

$$\mathbf{H} = \sqrt{\frac{K}{1+K}} \mathbf{G} + \sqrt{\frac{1}{1+K}} \mathbf{R}^{1/2} \mathbf{W} \mathbf{T}^{1/2}, \quad (2)$$

where K is the Rician K -factor, \mathbf{G} is the $N_r \times N_t$ line-of-sight (LOS) channel component matrix, \mathbf{W} is the $N_r \times N_t$ matrix of scattered channel components, and \mathbf{R} and \mathbf{T} are the $N_r \times N_r$ receive

and $N_t \times N_t$ transmit antenna correlation matrices respectively. The elements of the LOS channel matrix \mathbf{G} are given as [8]

$$G_{i,j} = \exp\left(\frac{j2\pi}{\lambda}L_{i,j}\right), \quad (3)$$

where λ is the wavelength and $L_{i,j}$ is the physical distance between transmit antenna j and receive antenna i . In [8], $L_{i,j}$ is approximated as

$$L_{i,j} \approx R + \Delta_y + \frac{\Delta_x^2 + \Delta_z^2}{2R}, \quad (4)$$

where Δ_x , Δ_y , and Δ_z represent the distance between the transmit antenna j and receive antenna i in the respective directions when disregarding the distance between the transmit and receive arrays. This approximation is very accurate for cases where $R \gg \Delta_x, \Delta_y, \Delta_z$ [8]. Due to the antenna arrays being constrained to x - z planes, $\Delta_y = 0$ in all cases. Thus, equation (3) becomes

$$G_{i,j} \approx \exp\left(\frac{j2\pi}{\lambda}\left[R + \frac{\Delta_x^2 + \Delta_z^2}{2R}\right]\right), \quad (5)$$

The elements of \mathbf{R} and \mathbf{T} express the correlations between the receive and the transmit antenna pairs, calculated for antennas i and j as

$$R_{i,j} = \alpha_r \binom{d_{i,j}}{d_r} \quad \text{and} \quad T_{i,j} = \alpha_t \binom{d_{i,j}}{d_t}, \quad (6)$$

where α_r and α_t represent the correlation between neighboring antennas in the receive and transmit antenna arrays respectively, and $d_{i,j}$ is the physical distance between the positions of antenna i and antenna j within the transmit array or the receive array.

The channel matrix \mathbf{H} is assumed to be known both at the transmitter and the receiver. The receiver employs the maximum likelihood (ML) detector as

$$\hat{\mathbf{u}} = \underset{\mathbf{u}}{\operatorname{argmin}} \|\mathbf{y} - \mathbf{H}\mathbf{u}\|_2^2, \quad (7)$$

where $\hat{\mathbf{u}}$ is the detected GSM symbol.

MASSIVE MIMO SYMBOL DESIGN

We begin by describing block generalized spatial modulation (BGSM) symbols. In the BGSM symbols, b antennas are grouped together into an antenna block as shown in Fig. 2. Note that, for the sake of simplicity, we restrict our study to cases where N_t is evenly divisible by b and there is no overlap between antenna blocks as shown in Fig. 2 (a). Each antenna block requires only one RF transmit chain since the same QAM symbol is transmitted by all the antennas in any given block. We denote N'_a as the number of RF transmit chains, or equivalently the number of active antenna blocks. A BGSM symbol is represented by $\mathbf{v} = [v_1, \dots, v_{N'_t}]^T$, where $N'_t = N_t/b$ is the number of available antenna blocks, v_i is the symbol transmitted by the i -th antenna block, $v_i \in \mathcal{B}$ if the i -th antenna block is active, and $v_i = 0$ for the remaining $N'_t - N'_a$ antenna blocks. Thus, the number

of antennas activated when a symbol \mathbf{v} is transmitted is $N_a = bN'_a$. Note that for the case where $b = 1$, BGSM is equivalent to GSM.

There are $C = M^{N'_a} \binom{N'_t}{N'_a}$ total BGSM symbols to choose from, and we denote \mathcal{U} as the set of available BGSM symbols. When a spectral efficiency of r is desired, a set of $C' = 2^r$ symbols must be chosen to be used for communication. Since typically $C > C'$, there are $\binom{C}{C'}$ available options. An exhaustive search through these options is numerically too complex. The work in [5] presents an ICGSM algorithm to lower the complexity of the symbol set selection problem. The ICGSM algorithm is later adapted to RF MIMO systems in [10].

We now describe the BICGSM algorithm for large MIMO systems. The steps of the BICGSM

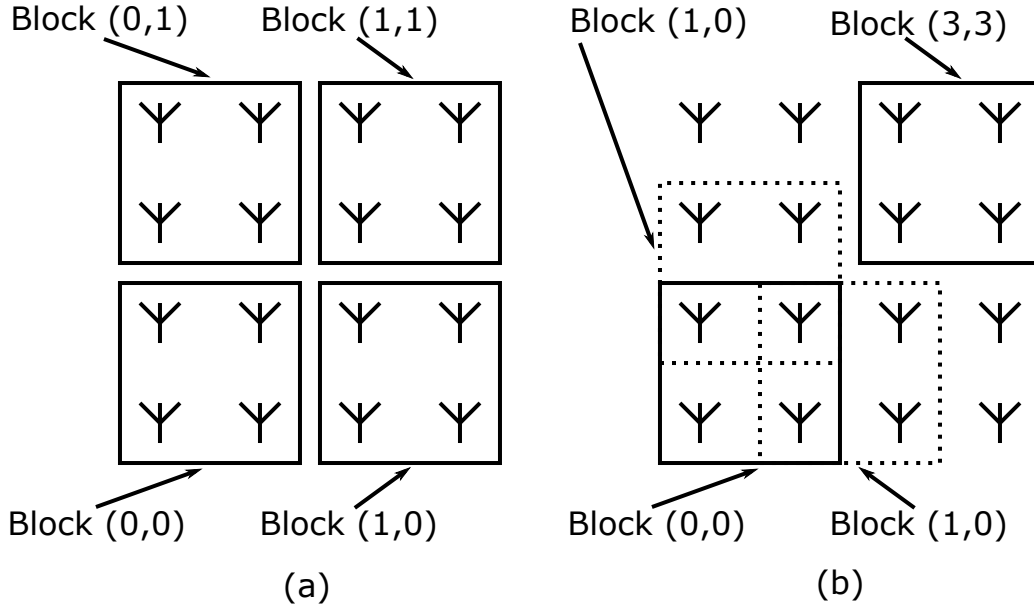


Figure 2: An example of antenna grouping in a BGSM system with $b = 4$. Two possible blocking approaches are shown: (a) no overlap of antenna blocks, and (b) overlapping antenna blocks.

algorithm are summarized in the following steps.

1. **Select a set of BGSM symbols:** Select a BGSM symbol set Ω with $|\Omega| = 2^r$ and create the complementary set $\Lambda = \mathcal{U} \setminus \Omega$. The set Ω can be randomly selected, or selected based on simple tests.
2. **Move a BGSM symbol from the complimentary set to the symbol set:** Move the first BGSM symbol from Λ to the set Ω to create the set Ω' with $|\Omega'| = 2^r + 1$.
3. **BGSM symbol removal:** Calculate the inter-symbol distance $D_{i,j}$ for each BGSM symbol pair $(\mathbf{v}_i, \mathbf{v}_j)$, $\mathbf{v}_i, \mathbf{v}_j \in \Omega'$. It is shown in [10] that using $E[D_{i,j}^2]$ in place of $D_{i,j}$ in the symbol design improves performance for Rician fading RF systems, since $E[D_{i,j}^2]$ considers both the LOS and scattered channel components \mathbf{G} and \mathbf{W} . Note that each BGSM symbol \mathbf{v}_i uniquely maps to a GSM symbol \mathbf{u}_i , which is used for inter-symbol distance calculations. Thus, $E[D_{i,j}^2]$ can be calculated as

$$E[D_{i,j}^2] = \frac{K}{1+K} \|\mathbf{G}(\mathbf{u}_i - \mathbf{u}_j)\|_2^2 + \frac{N_r}{1+K} (\mathbf{u}_i - \mathbf{u}_j)^H \mathbf{T} (\mathbf{u}_i - \mathbf{u}_j). \quad (8)$$

Identify and remove the BGSMSymbol whose removal provides the highest minimum $E[D_{i,j}^2]$ among the remaining BGSMSymbols to create the set Ω . Update Λ .

4. **Iteration:** Return to Step 2 and repeat this process by choosing the next BGSMSymbol in Λ until a stopping criterion is met.

Note that when a symbol moved to Ω results in performance degradation, it gets removed in the same iteration. Thus, the BICGSM algorithm can only improve the performance of the initial set. The BICGSM algorithm significantly reduces complexity in comparison to the ICGSM algorithm. Whereas the ICGSM algorithm for GSM symbols must search among $M^{N_a} \binom{N_t}{N_a}$ GSM symbols, the BICGSM algorithm only has to search among $M^{N'_a} \binom{N'_t}{N'_a}$ BGSMSymbols. In addition to reducing complexity, the BICGSM algorithm also outperforms ICGSM when the two algorithms are compared with an equal number of RF transmit chains N'_a . However, when compared in terms of equal number of active antennas N_a , the ICGSM algorithm outperforms the BICGSM algorithm.

NUMERICAL RESULTS

We now investigate the SER performance and complexity of the BICGSM algorithm for various scenarios. For all of our numerical results, we use $N_r = 2$, $M = 4$ (e.g. QPSK), $\alpha_t = \alpha_r = 0.5$, $R = 100$ m, $d_t = d_r = \lambda/2$, and $r = 3$ bpcu. The signal-to-noise ratio (SNR) is defined as $\text{SNR} = \gamma^2 b N'_a E_s / \sigma^2$, where E_s is the average symbol energy of the QAM alphabet. The URA transmitter array configuration is used.

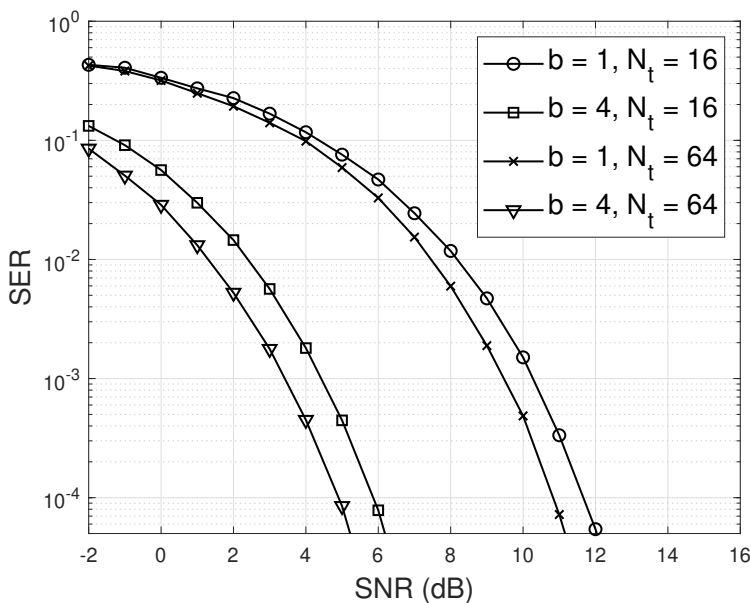


Figure 3: The SER performance of the BICGSM algorithm for LOS channel ($K = \infty$) when N'_a is fixed at 2.

In Fig. 3, the SER performance of the BICGSM is shown with $b \in \{1, 4\}$ and $N_t \in \{16, 64\}$. We use an LOS channel ($K = \infty$) and $N'_a = 2$ in all curves. The comparison is fair in the

sense of using the same number of RF transmit chains. The BICGSM algorithm offers the best performance for $b = 4$ and $N_t = 64$. A gain of 1 dB is obtained over the case with $b = 4$ and $N_t = 16$. In comparison to the cases with $b = 1$, the BICGSM with $b = 4$ offers a gain of 6 dB for both $N_t = 16$ and $N_t = 64$. The case with $b = 1$ and $N_t = 64$ involves a search over 32,256 possible symbols, whereas the case with $b = 4$ and $N_t = 64$ only requires a search over 1,920 symbols. Thus, the figure demonstrates that the BICGSM algorithm can improve SER performance while simultaneously reducing complexity. The BICGSM algorithm is able to provide a gain over the ICGSM algorithm due to the increased array gain of the multiple active antennas in an active antenna block. This gain increases when a larger number of transmit antennas is used as shown in Fig. 3.

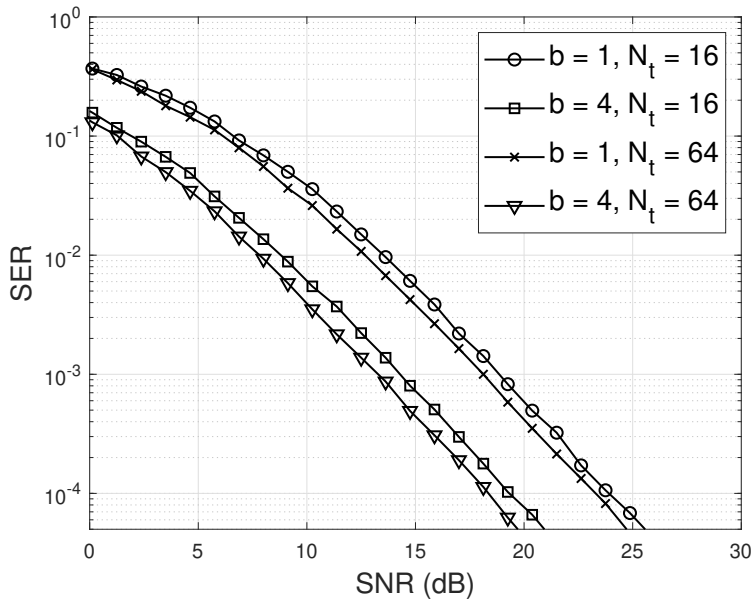


Figure 4: The SER performance of the BICGSM algorithm for a partially scattered channel. We use $K = 1$.

We investigate the error performance of the BICGSM algorithm in a Rician channel in Fig. 4. We use $K = 1$, which indicates a channel where the received power is distributed equally through the LOS and scattered channel components \mathbf{G} and \mathbf{W} . The rest of the parameters are the same as in Fig. 3. The case with $N_t = 64$ and $b = 4$ offers the best performance again. The cases with $b = 4$ offer a gain of 5 dB over the cases with $b = 1$ for the same number of transmit antennas N_t . Comparing Fig. 4 to Fig. 3, the SER in the Rician channel is higher for the same SNR. Additionally, the gains offered by the $b = 4$ cases decrease slightly. This is because the increased array gain within the LOS channel matrix component \mathbf{G} is diminished by the random perturbations of the equally powerful scattered channel matrix component \mathbf{W} .

The BICGSM algorithm offers better error performance than the ICGSM algorithm when compared with equal N'_a because the BICGSM algorithm benefits from increased array gain due to having $N_a = bN'_a$ antennas active in comparison to the $N_a = N'_a$ active antennas in ICGSM. In Fig. 5, we consider selections of b and N'_a such that the ICGSM (e.g. $b = 1$) and the BICGSM algorithms use the same number of active antennas N_a . The figure uses $N_t = 16$, $K = 5$, and $N_a = 4$. We

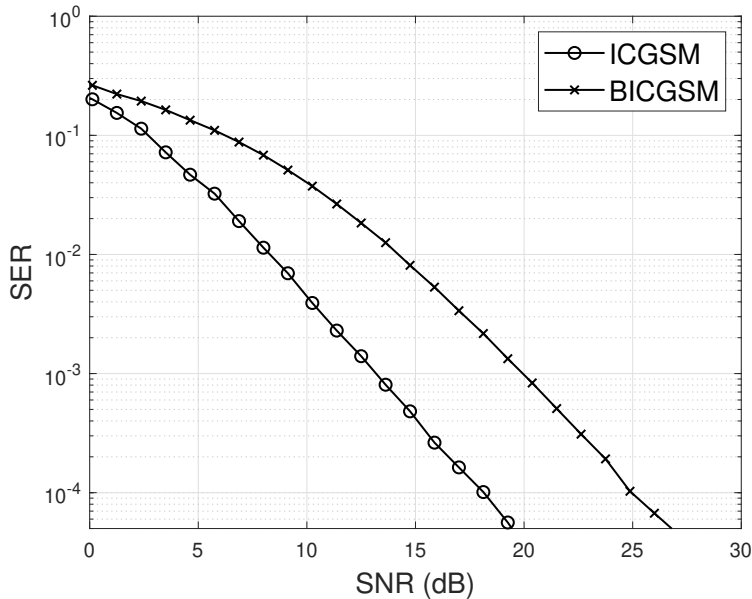


Figure 5: The performance of the ICGSM algorithm ($b = 1$, $N'_a = 4$) is compared against the performance of the BICGSM algorithm ($b = 4$, $N'_a = 1$) with the same number of activated antennas in both algorithms. We use $N_a = 4$, $N_t = 16$, and $r = 3$ bpcu.

fix $N_a = 4$ by choosing $b = 4$ and $N'_a = 1$ for the BICGSM algorithm, and $b = 1$ and $N'_a = 4$ for the ICGSM algorithm. The rest of the parameters are the same as in Fig. 3. The ICGSM algorithm significantly outperforms the BICGSM algorithm. This is to be expected as the ICGSM algorithm allows all N_a active antennas to select different QAM symbols, while the BICGSM is restricted to a block of antennas all transmitting the same symbol. Consequently, the ICGSM algorithm incurs much higher complexity to solve this case than the BICGSM algorithm. The ICGSM algorithm needs to search over 465,920 symbols, a process which can require millions of iterations within the ICGSM algorithm. This means that the ICGSM algorithm is impractical for larger systems that require a quick symbol set design, whereas the BICGSM can reduce this prohibitive complexity significantly at the cost of SER performance.

We investigate the error performance of the BICGSM algorithm when used for a massive MIMO system in Fig. 6. The figure uses $N_t = 256$, $N'_a = 2$, and $K = 5$. We vary the BICGSM block size with $b = 4, 16$, and 64 . The case where $b = 64$ yields the best performance by about 5 dB over the case with $b = 16$. This is because the $b = 64$ case uses more active antennas and benefits from increased array gain. The $b = 64$ case also offers much lower complexity than the other two cases. Finally, Fig. 7 shows the available number of symbols for $b = 1, 4$, and 16 . Therefore, a symbol search algorithm has to search over these symbols. We use $M = 4$ and $N'_a = 2$. As the block size used in the BICGSM increases, the complexity of the symbol set selection problem decreases drastically. This can make it possible to solve scenarios that are otherwise infeasible to solve.

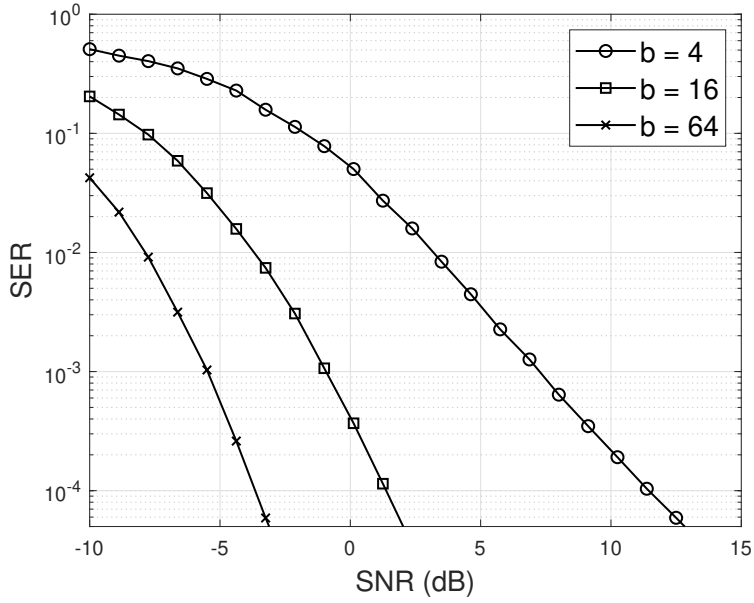


Figure 6: The SER performance of the BICGSM algorithm for a massive MIMO system with $N_t = 256$.

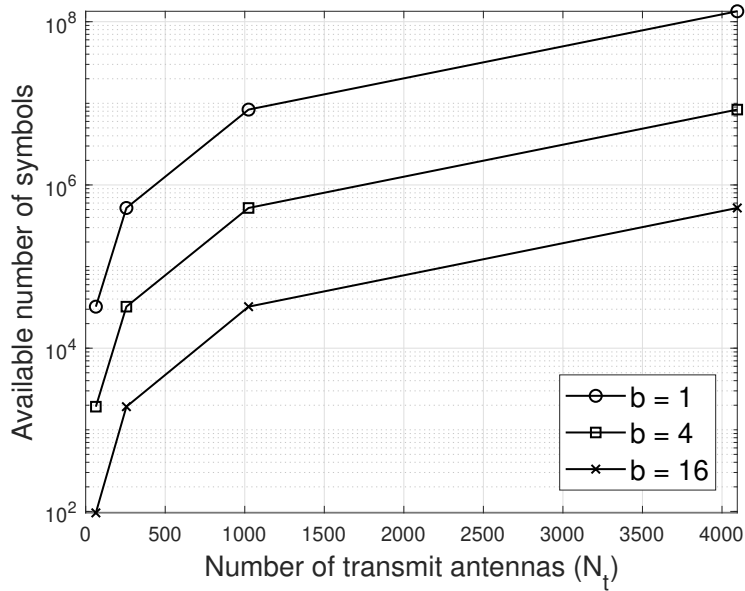


Figure 7: Complexity of the symbol search process.

CONCLUSION

The BICGSM algorithm is developed to lower the complexity of the GSM symbol set selection problem for massive MIMO RF systems with Rician fading and correlated antennas. The SER performance and complexity of the BICGSM are investigated for a variety of scenarios and antenna configurations. The BICGSM algorithm is found to significantly reduce the complexity of the sym-

bol set selection problem. The BICGSM is capable of providing better SER performance than the ICGSM algorithm when using the same number of transmitter processing chains. When compared to the ICGSM with the same number of total active antennas, the BICGSM algorithm is shown to provide much lower complexity at the cost of SER performance. The algorithm is shown to be well suited to large scale MIMO systems and allows for fast symbol set design in comparison to existing symbol design methods.

REFERENCES

- [1] J. Zeng, J. Lin, and Z. Wang, "Low complexity message passing detection algorithm for large-scale MIMO systems," *IEEE Wireless Communications Letters*, vol. 7, pp. 708–711, Oct 2018.
- [2] N. Garcia, H. Wymeersch, E. G. Larsson, A. M. Haimovich, and M. Coulon, "Direct localization for massive MIMO," *IEEE Transactions on Signal Processing*, vol. 65, pp. 2475–2487, May 2017.
- [3] Y. Sun, D. K. Borah, and E. Curry, "Optimal symbol set selection in GSSK visible light wireless communication systems," *IEEE Photonics Technology Letters*, vol. 28, pp. 303–306, Feb. 2016.
- [4] E. Curry, D. K. Borah, and J. M. Hinojo, "Optimal symbol set design for generalized spatial modulations in MIMO VLC systems," in *IEEE Globecom, 2016*, pp. 1–7, Washington, D.C., Dec 2016.
- [5] E. Curry and D. K. Borah, "Iterative combinatorial symbol design for spatial modulations in MIMO VLC systems," *IEEE Photonics Technology Letters*, vol. 30, pp. 483–486, March 2018.
- [6] G. Taricco and E. Riegler, "On the ergodic capacity of correlated rician fading MIMO channels with interference," *IEEE Transactions on Information Theory*, vol. 57, pp. 4123–4137, July 2011.
- [7] C. Liu and R. Malaney, "Location-based beamforming and physical layer security in Rician wiretap channels," *IEEE Transactions on Wireless Communications*, vol. 15, pp. 7847–7857, Nov. 2016.
- [8] F. Bøhagen, P. Orten, and G. Øien, "Optimal design of uniform rectangular antenna arrays for strong line-of-sight MIMO channels," *EURASIP Journal on Wireless Communications and Networking*, vol. 2007, p. 045084, Aug. 2007.
- [9] R. B. Ertel, P. Cardieri, K. W. Sowerby, T. S. Rappaport, and J. H. Reed, "Overview of spatial channel models for antenna array communication systems," *IEEE Personal Communications*, vol. 5, pp. 10–22, 1998.
- [10] E. Curry and D. K. Borah, "Generalized spatial modulation symbol design for correlated rician fading MIMO channels," in *Proc. International Telemetering Conference*, Glendale, AZ, Nov. 2018.